Observation of an unconventional metal-insulator transition in overdoped CuO_2 compounds

F. Venturini¹, M. Opel¹, T. P. Devereaux², J. K. Freericks³, I. Tüttő⁴,
B. Revaz⁵, E. Walker⁵, H. Berger⁶, L. Forró⁶, and R. Hackl¹

¹Walther Meissner Institute, Bavarian Academy of Sciences, 85748 Garching, Germany

²Department of Physics, University of Waterloo, Waterloo, Ontario Canada N2L 3G1

³Department of Physics, Georgetown University, Washington, DC 20057, U.S.A.

⁴RISPO, Hungarian Academy of Sciences, P.O.Box 49, 1525 Budapest, Hungary

⁵DPMC, University of Geneva, 1121 Genève, Switzerland and

⁶EPFL, Ecublens, 1025 Lausanne, Switzerland

(Dated: October 27, 2018)

The electron dynamics in the normal state of $\mathrm{Bi_2Sr_2CaCu_2O_{8+\delta}}$ is studied by inelastic light scattering over a wide range of doping. A strong anisotropy of the electron relaxation is found which cannot be explained by single-particle properties alone. The results strongly indicate the presence of an unconventional quantum-critical metal-insulator transition where "hot" (antinodal) quasiparticles become insulating while "cold" (nodal) quasiparticles remain metallic. A phenomenology is developed which allows a quantitative understanding of the Raman results and provides a scenario which links single- and many-particle properties.

PACS numbers: 74.72.-h, 33.20.fb, 74.20.F

The normal state of copper-oxygen compounds is characterized by several crossover lines separating regions of the phase diagram with different physical properties. [1] The line usually identified with the opening of a pseudogap at T^* has been observed in many experiments which probe both single-particle properties such as specific heat, angle-resolved photoemission (ARPES), and many-particle properties such as NMR and transport. [2, 3] An additional crossover at higher temperatures and doping has been determined from anomalies in NMR at T_0 . [4] Moreover, another temperature scale T_{MI} associated with a metal-insulator transition has been found in transport. [5] Although several scenarios have been proposed [6, 7, 8, 9, 10, 11, 12] there is no consensus of whether and how T^*, T_0 and T_{MI} are related. It would be extremely useful if a description of electron dynamics could be able to connect the results from various experiments to a common origin.

From the point of view of critical phenomena it is not uncommon that single-particle properties may show substantially different behavior from many-particle properties. [13] In the vicinity of a quantum phase transition (QPT) single-particle properties, e.g., density of states at the Fermi level may be uncritical while two-particle properties such as the conductivity may deviate from Fermi liquid behavior. For studying a putative QPT in planar anisotropic systems like the copper-oxygen compounds a method is desirable which not only probes many-particle properties but also has resolution in k space. Raman scattering of light by electrons can indeed meet these requirements in that the dynamical response can be measured for different regions in the Brillouin zone due to the possibility to independently adjust the polarizations of incoming and outgoing photons. Thus, the B_{1g} and B_{2g}

electronic Raman spectra can probe either "hot" (antinodal) or "cold" (nodal) electrons with momenta along the principal axes and the diagonals of the CuO₂ plane, respectively.

In this paper we present results from Raman scattering experiments in ${\rm Bi_2Sr_2CaCu_2O_{8+\delta}}$ (Bi2212) over a wide range of effective doping 0.09 . We show that the transport of "hot" electrons vanishes already at very high doping levels while the "cold" ones still display metallic behavior. We propose a phenomenology which can describe the results quantitatively and outline how the various regimes in the phase diagram could be connected.

The experiments have been performed on a set of single crystals with different doping levels. We started from an extremely homogeneous overdoped Bi2212 crystal grown by the traveling solvent floating zone (TSFZ) method with a T_c of 78 K and a transition width of only 0.2 K. From this specimen several pieces were cut and annealed at 620 K in oxygen partial pressures of 300 and 1350 bar to obtain transition temperatures of 62 and 56 K, respectively.

Raw data of the Raman response $\chi''_{\mu}(\omega, T, p)$ (with the symmetry index $\mu = B_{1g}, B_{2g}$) for various temperatures are plotted in Fig. 1. Superimposed on the broad electronic continua are narrow bands originating from Raman-active lattice vibrations. The overall continua for B_{2g} symmetry (bottom row) are relatively doping independent and show a low-energy response, $\omega < 200 \text{ cm}^{-1}$, which decreases with increasing T. In contrast, for B_{1g} symmetry (top row) the continua show non-trivial dependence on doping and T: the low-energy response decreases with increasing T in a similar way as in B_{2g} symmetry for the strongly overdoped sample (Fig. 1 (e)),

becomes temperature independent near optimum doping $p \geq 0.16$ (Fig. 1 (c)), and increases with increasing T for samples below optimum doping (Fig. 1 (a)). The different doping dependences for the two symmetries become strikingly evident if the spectra are plotted at a fixed temperature $T \simeq 180$ K as a function of carrier concentration p as shown in Fig. 2. For B_{2g} symmetry (Fig. 2 (b)) the doping dependence is very weak. For B_{1g} symmetry (Fig. 2 (a)) the response is suppressed strongly with decreasing doping in an energy range of about 2000 cm⁻¹ indicating the existence of a gap of this magnitude for the "hot" electrons.

In order to link the results to momentum-dependent electron dynamics we analyze the electronic Raman response in the dc limit, $\omega \to 0$. For non-resonant scattering we obtain [14]

$$\chi''_{\mu}(\ \omega \to 0) = \omega N_F \times \times \left\langle \gamma_{\mu}^2(\mathbf{k}) \int d\xi \left(-\frac{\partial f^0}{\partial \xi} \right) \frac{Z_{\mathbf{k}}^2(\xi, T)}{2\Sigma_{\mathbf{k}}''(\xi, T)} \right\rangle. \tag{1}$$

Here N_F is the density of electronic levels at the Fermi energy E_F and $\gamma_{\mu}(\mathbf{k})$ is the Raman scattering amplitude, dependent upon incident (scattered) photon polarizations $\hat{e}_{I(S)}$ corresponding to different symmetries $\mu = B_{1g}, B_{2g}$. $\Sigma''_{\mathbf{k}}$ is the imaginary part of the single-particle self energy related to the electron lifetime as $\hbar/2\Sigma''_{\mathbf{k}}(\omega,T) = \tau_{\mathbf{k}}(\omega,T)$, $Z_{\mathbf{k}}(\omega,T)$ is the quasiparticle residue, f^0 is the Fermi distribution function, and $\langle \cdots \rangle$ denotes an average over the Fermi surface.

Using Eq. (1) we can define the Raman relaxation rate via the slope of the spectra in the dc limit, $\Gamma_{\mu}(T) \equiv N_F \langle \gamma_{\mu}^2(\mathbf{k}) \rangle [\partial \chi_{\mu}''(\omega \to 0, T)/\partial \omega]^{-1}$. For an isotropic conventional metal one obtains $\Gamma_{\mu}(T) = \hbar/\tau(T)$. In a correlated or a disordered metal, however, a finite energy might be necessary to move an electron from one site to another one. Thus, in spite of a non-vanishing density of states at the Fermi level as observed in an ARPES experiment for instance no current can be transported and $\Gamma_{\mu}(T) \gg \hbar/\tau(T)$.

 $\Gamma_{\mu}(T)$ can be explicitly extracted from the Raman spectra by employing a memory or relaxation function approach. [15, 16] In Fig. 3 (a) Raman relaxation rates at a fixed temperature T = 200 K obtained in this and previous studies [15] are compiled. The magnitude of $\Gamma_{B_{1g}}$ decreases by approximately 70% for 0.09 $\leq p \leq$ 0.22, while $\Gamma_{B_{2q}}$ is almost constant up to $p \simeq 0.20$ and changes by only 30% in the narrow range 0.20 .The abrupt crossover for 0.20 is remarkable:the Raman relaxation rates rapidly decrease, and the anisotropy vanishes. We emphasize that the changes for 0.20 are observed for a set of samples preparedfrom a single homogeneous piece and that the results agree well with those from earlier experiments, hence the observed features are robust. The variations of the relaxation rates with temperature $\partial \Gamma_{\mu}(T)/\partial T$ are shown in

Fig. 3(b). $\partial \Gamma_{B_{2g}}(T)/\partial T$ (nodal electrons) deviates only little from 2 in the entire doping range. The logarithmic derivative $\partial [\ln \Gamma_{B_{2g}}(T)]/\partial (\ln T)$ [Fig. 3(c)] demonstrates that $\Gamma_{B_{2g}}(T)$ varies essentially linearly with temperature. The two properties combined yield $\Gamma_{B_{2g}}(T) \simeq 2k_BT$. In contrast, both $\partial \Gamma_{B_{1g}}(T)/\partial T$ and $\partial (\ln \Gamma_{B_{1g}}(T))/\partial (\ln T)$ (anti-nodal electrons) are strongly temperature dependent, increase continuously with p and change sign close to optimum doping. For $p \geq 0.22$ any kind of anisotropy disappears.

It is both the apparent symmetry dependence of the Raman relaxation rates, $\Gamma_{B_{2g}} < \Gamma_{B_{1g}}$, [Fig. 3 (a)] and their characteristic increase towards lower temperature, $\partial \Gamma_{B_{1g}}(T)/\partial T < 0$ for $p \leq 0.16$ [Fig. 3 (b)] which indicate that there is not only gap-like behavior but also a strong anisotropy of the gap with the maxima located around the M-points (see Fig. 1 (e,f) and 3 (a)). Thus the "hot" electrons show a crossover from metallic to insulating behavior near optimum doping while the "cold" ones are metallic for all doping levels at the temperatures examined. This is what we call an anisotropic or generalized metal-insulator transition (MIT) as opposed to a conventional Mott transition [17] since the charge excitations become gapped only on parts of the Fermi surface, and the overall dc transport is still metallic.

The momentum dependence of the gap is reminiscent of both the superconducting gap and the pseudogap [2, 3] being compatible with $\mid d_{x^2-y^2} \mid$ symmetry. In spite of a similar **k** dependence, however, an incipient superconducting instability (pre-formed pairs) can be safely excluded because of the high temperature (200 K) and doping level (p>0.19) of our experiment. The same holds for the pseudogap. Its onset temperature T^* actually merges with T_c already for 0.16 . [2, 3] The scenario we have in mind here is that of an anisotropic charge gap which develops near the "hot" spots to minimize strong interactions between electrons. [18] Therefore, we examine the effect of an anisotropic normal-state gap on the Raman response.

An exact treatment of non-resonant electronic Raman scattering in systems displaying a quantum-critical MIT in the limit of infinite dimensions has been formulated for Hamiltonians displaying both Fermi-liquid and non-Fermi-liquid ground states. [19] However, the nature of a MIT in physical dimensions, the development of an anisotropic gap, and their effect on the Raman response is still an open issue. Rather than speculating on what drives the QPT we consider here a phenomenological treatment for a system near a QPT possessing a dopingdependent anisotropic gap in the charge channel $\Delta_{\rm C}(p)$. The result can be directly derived from Eq. (1) using the following approximations: (1) we assume that the wavefunction renormalization factor is constant, $Z_{\mathbf{k}}(\omega, T) \equiv$ Z, and non-zero only for $\Delta_{\rm C} \leq |2\hbar\omega| \leq E_{\rm b}$, e.g., for frequencies located in either part of the band with a total width $E_{\rm b}$ separated symmetrically with respect to

the chemical potential by $\pm \Delta_{\rm C}/2$, [20] (2) we take the imaginary part of the self energy to be momentum, energy, and doping independent, $\Sigma_{\bf k}''(\omega,T)=\Sigma''(T)$, (3) we assume a simple momentum dependence of the gap which is compatible with the observed **k**-dependence, $\Delta_{\rm C}({\bf k},p)=\Delta_{\rm C}(\varphi,p)\equiv \Delta_{\rm C}^0(p)\cos^2(2\varphi)$ with φ the azimuthal angle on a cylindrical Fermi surface, and (4) the doping dependence of the gap is postulated to be proportional to $(1-p/p_c)^{\zeta}$ for $p\leq p_c$. We obtain for $\Delta_{\rm C}(p),k_BT\ll E_{\rm b}$

$$\frac{\Gamma_{\mu}(p,T)}{2\Sigma''(T)} = \begin{cases} \frac{1}{2} \left[1 + \exp\left(\frac{\Delta_{\mathbf{C}}^{\mu}(p)}{2k_{B}T}\right)\right] \text{ (insulator)}, \\ 1 \text{ (metal)}. \end{cases}$$
 (2)

 $\Delta^{\mu}_{\mathrm{C}}(p)$ is a symmetry-specific effective gap resulting from the Fermi-surface integration using $\gamma_{B_{1g}}(\varphi) \sim \cos(2\varphi)$, and $\gamma_{B_{2g}}(\varphi) \sim \sin(2\varphi)$.

In Fig. 3 along with the data, we plot theoretical curves calculated from Eq. (2) using $\Sigma''(T) = k_B T$ (being qualitatively compatible with ARPES results in a wide range of doping [21]), $\Delta_{\rm C}^0/k_B = 1100$ K, and $\zeta = 0.25$. For the B_{2q} symmetry which, according to our previous studies, reflects dc and optical transport properties [15], the influence of the gap is weak, and the temperature dependence comes essentially from $\Sigma''(T)$. The general trend of the B_{1q} rates, in particular the sign change, is well reproduced by the phenomenology. It cannot be derived from single-particle properties which, to our present knowledge, depend only negligibly on doping in the range studied. [22] Due to the selection rules or, equivalently, the weighted Fermi surface average (Eq. (1)) the MIT is particularly well resolved in the Raman experiment and can be observed clearly up to its onset at $p \simeq 0.22$.

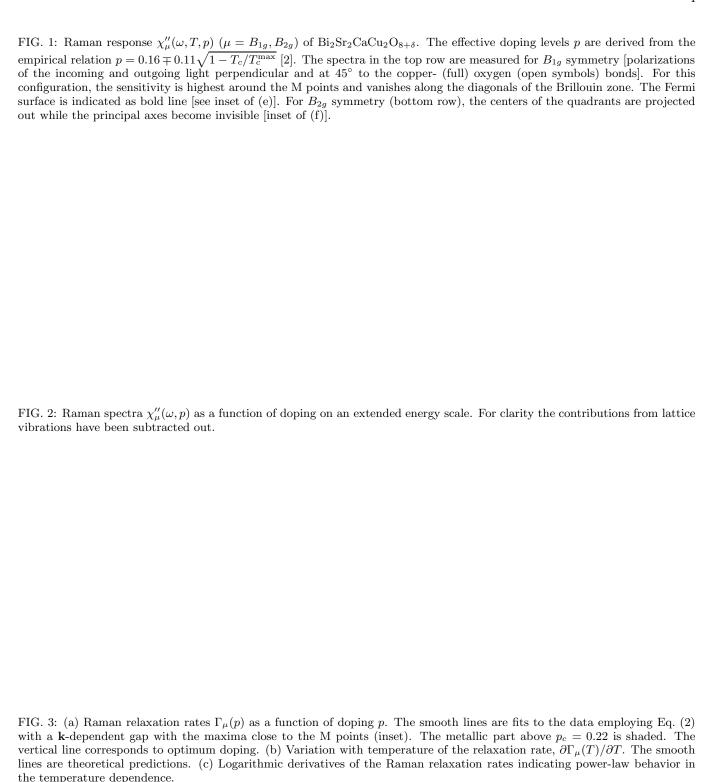
This strongly suggests that an underlying quantum critical point for this material lies at a doping of $p_c \simeq 0.22$ which is considerably higher than $p_c^{tr} \simeq 0.19$ as derived from transport properties. [2, 3, 5] Nevertheless, it appears that the two phenomena are directly linked. The differences in the critical doping in transport and Raman can readily be traced back to the selection rules and directly reflect the unconventional anisotropic nature of the transition. Since $p_c \simeq 0.22$ is also inferred from the T_0 line [1] Raman scattering probably captures the first onset of non Fermi liquid behavior in this compound and can trace it back to a correlation-induced localization of carriers. On the other hand, the pseudogap at T^* does not fit straightforwardly into this scenario. It is either marks a pairing or charge-ordering instability or is connected to T_0 in a more complicated way through the electron-phonon interaction. [10]

The existence of a QPT seems to be a general feature of the cuprates although the critical doping depends on the material class as demonstrated for low T_c compounds. [5] Here we have shown that the QPT can be described phenomenologically in terms of a generalized MIT with a strongly anisotropic gap. In this framework

the Raman data can be explained quantitatively and reconciled with the single-particle results from ARPES. Why p_c is smaller in systems with lower T_c 's remains an important question.

Many clarifying discussions with B.S. Chandrasekhar, D. Einzel and A. Virosztek are gratefully acknowledged. F.V. is indebted to the Gottlieb Daimler-Karl Benz Foundation for financial support. The work is part of the DFG project under grant number HA2071/2-1. J.K.F. acknowledges support from N.S.F. under grant number DMR-9973225.

- [1] M. Gutmann, E.S. Božin, S.J.L. Billinge, cond-mat 0009141 (2000).
- [2] J.L. Tallon and J.W. Loram, Physica C **349**, 53 (2001).
- [3] T. Timusk and B.W. Statt, Rep. Prog. Phys. 62, 61 (1999).
- [4] H. Alloul, T. Ohno, and P. Mendels, Phys. Rev. Lett. 63, 1700 (1989).
- [5] Y. Ando et al., Phys. Rev. Lett. 75, 4662 (1995); 77, 2065 (1996); 79, 2595 (1997); Phys. Rev. B 56, R8530 (1997); G. S. Boebinger et al., Phys. Rev. Lett. 77, 5417 (1996); P. Fournier et al., ibid 81, 4720 (1998); S. Ono et al., ibid 85, 638 (2000).
- [6] J. Zaanen and O. Gunnarsson, Phys. Rev. B 40, 7391 (1989).
- [7] A. Sokol and D. Pines, Phys. Rev. Lett. 71, 2813 (1993).
- [8] V. Emery and S. Kivelson, Nature **374**,434 (1995).
- [9] S.C. Zhang, Science **275**, 1089 (1997).
- [10] S. Andergassen et al., Phys. Rev. Lett. 87, 56401 (2001).
- [11] C.M. Varma, Phys. Rev. B 61, R3804 (2000)
- [12] S. Chakravarty et al., Phys. Rev. B 63, 094503 (2001).
- [13] S. Sachdev, Science 288, 475 (2000).
- [14] T.P. Devereaux and A.P. Kampf, Phys. Rev. B 59, 6411 (1999).
- [15] M. Opel et al., Phys. Rev. B 61, 9752 (2000).
- [16] J.G. Naeini et al., Can. J. Phys. 5-6, 483 (2000).
- [17] N. Mott, Conduction in Non-Crystalline Materials (Clarendon Press, Oxford, 1987).
- [18] N. Furukawa et al., Phys. Rev. Lett. 81, 3195 (1998); J. González et al., Phys. Rev. Lett. 84, 4930 (2000).
- [19] J. K. Freericks and T. P. Devereaux, Phys. Rev. B 64, 125110 (2001); J. K. Freericks, T. P. Devereaux, and R. Bulla, Phys. Rev. B 64, 233114 (2001).
- [20] As shown for a marginal Fermi liquid, for instance, Z=0 does not necessarily imply that one cannot observe a Fermi surface. The approximation is therefore not in conflict with ARPES. In general, the gap $\Delta_{\rm C}$ should be considered an activation energy for moving a particle rather than a single particle gap.
- [21] M.R. Norman, M. Randeria, H. Ding, and J.C. Campuzano, Phys. Rev. B 57, R11093 (1998); T. Valla, A.V. Fedorov, P.D. Johnson, Q. Li, G.D. Gu, and N. Koshizuka, Phys. Rev Lett. 85, 828 (2000).
- [22] A.A. Kordyuk et al., cond-mat/0201485 (2001).



This figure "f1.gif" is available in "gif" format from:

http://arxiv.org/ps/cond-mat/0206210v1

This figure "f2.gif" is available in "gif" format from:

http://arxiv.org/ps/cond-mat/0206210v1

This figure "f3.gif" is available in "gif" format from:

http://arxiv.org/ps/cond-mat/0206210v1